Research on the mechanism of liquid film rim caused by the jet impact

Wang Ruixiang*[1], Sun Lei [2], Huang Yong [3]
[1]China Academy of Aerospace Aerodynamics, Beijing, China
[2]Sino-European Institute of Aviation Engineering, Civil Aviation University of China, Tianjin, China
[3]School of Energy and Power Engineering, Beihang University, Beijing, China
*Corresponding author email : 597288505@qq.com

Abstract
Liquid film will be produced when the liquid jet impacts onto a plate. The phenomenon plays an important role in the pre-film of the atomization of gas turbines. Researchers found that a special rim appears with the film, and explained it as hydraulic jump. It has been proved that the appearance of the rim does affect the atomization.
A liquid film generator is built to expose the typical shape of the liquid film rim with the help of the PLIF method during the experiment. It is found by the experiment that the cross-sectional shape of the rim is not a semicircle, but an irregular leaf. In addition, the cross-sectional shape of the rim is quite different from that of the typical hydraulic jump. The analysis of the rim is carried out, based on the experiment, to reveal the mechanism of the rim. In order to explain the formation of the leaf-shaped rim, the cross-sectional shape of the rim is divided into two arcs with different curvatures. It is also found that the rim is formed by various factors simultaneously, such as gravity, surface tension and viscosity. A semi-empirical model is established for the description of the rim.

Keywords
Plate impingement jet; Liquid film rim; PLIF method; Semi-empirical model

Introduction

Liquid film will be produced when the liquid jet impact onto a plate. The phenomenon plays an important role in the pre-film of the atomization of gas turbines and liquid-propellant rocket engines. It is wildly known that the liquid film will affect the atomization directly and affect the subsequent combustion indirectly[1]. Moreover, according to the observation of the experimental phenomenon[2], it is found that the liquid film is not a thin sheet, there is a rim around it[3]. The rim contains most of the fluid in the liquid film when the jet velocity is low[4], making it difficult to break-up or atomize. Some researchers defined the rim as the hydraulic jump[5], while some assumed the rim is a simple border with a circular cross section jump[6] and even observed the unstable fluctuations above the rim[7].
The study on the film formed by liquid jet impact onto a plate in this paper, contains both the experiment and mechanical analysis. The result of the experiment distinguishes between the liquid film rim formed by the jet impact and the rim formed by other similar methods. A semi-empirical model is established to describe and predict of the rim. Moreover, the shape and the size of rim are derived in the form of explicit equations, which reveal the formation mechanism of the film rim.

Experimental setup and operating conditions

To get a typical film with legible rim, a jet impinging system is established. The schematic experimental system is shown in **Figure** 1. A high pressure nitrogen cylinder is used to direct

the liquid from a reservoir to flow into a 1mm diameter nozzle steadily. A piece of intact film will appear, when the jet that came from the nozzle, is impinging onto a horizontal plate.
The acquisition of data mainly relies on the way of taking photos. A digital camera is right above the plate to obtain the width of the rim. The PLIF method is used to get the typical cross-sectional shape of the rim, with the help of a CCD camera and a Nd: YAG lamellar laser shown in **Figure 2.** The red light with the wavelength of 590 nm will be reflected, when the green laser with the wavelength of 532 nm shines into the transparent liquid. Meanwhile, the CCD camera has the capability to receive the light with the wavelength of 590 nm only with the help of the filter[8].

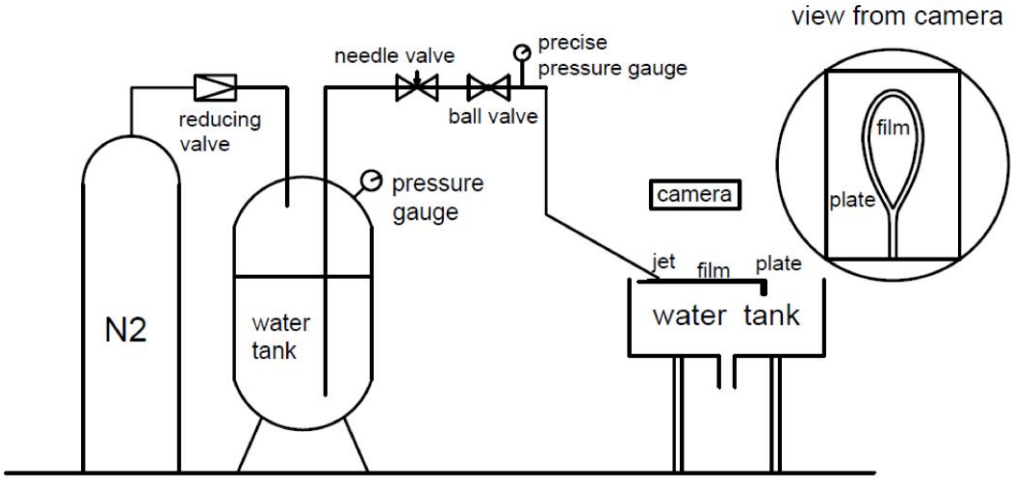

Figure 1. The layout of the primary test equipment.

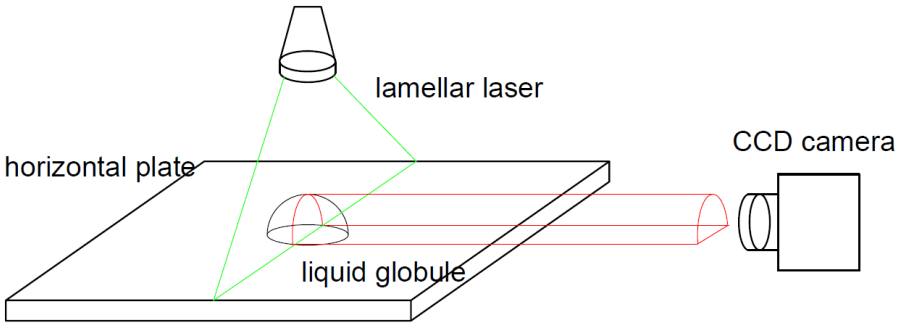

Figure 2. The layout of the primary PLIF equipment.

There are 3 primary operating conditions shown in **Table 1**. No.1 is the standard operating condition in which pure water is the working substance. No.2 magnified the dynamic viscosity, based on No.1. No.3 reduced the surface tension coefficient, based on No.1.

Table 1. Experimental operating conditions.

No	θ,°	V_0,m/s	ρ_l,kg/m^3	μ,mpa·s	σ_l,mN/m
1	30.0	9.6	1001.6	0.92	72.80
2	30.0	9.6	1142.8	9.51	68.53
3	30.0	9.6	1001.6	0.92	26.46

All the experiments shown in **Table 1** use the same horizontal plate made by plexiglass and the same nozzle made by aluminum. The processing accuracy of the plate is 1μm, so as to avoid the experimental error caused by the processing accuracy and the roughness of the surface. The orifice of the nozzle is drilled by laser, and the depth-diameter ratio is more than 10, so that the velocity profile of the jet that comes from the orifice, is fully developed Poiseuille flow. The whole experiment is carried out under 1 standard atmospheric pressure.
The velocity can be controlled by adjusting the needle valve, the impact angle can be controlled by adjusting the nozzle fix angle, the surface tension coefficient can be controlled by adjusting the concentration of inorganic salts in the liquid, the dynamic viscosity can be controlled by adjusting the concentration of glycerine in the liquid.

Typical phenomena

Figure 3 shows the typical film caused by the jet impact onto a horizontal plate. The leaf-shaped film is right spread on the plate, and is accompanied with the rim. The description of the film is shown in Wang[9], who divides the liquid film into two border lines(inner and outer border lines) and two zones(thin-layer and raised zone) .

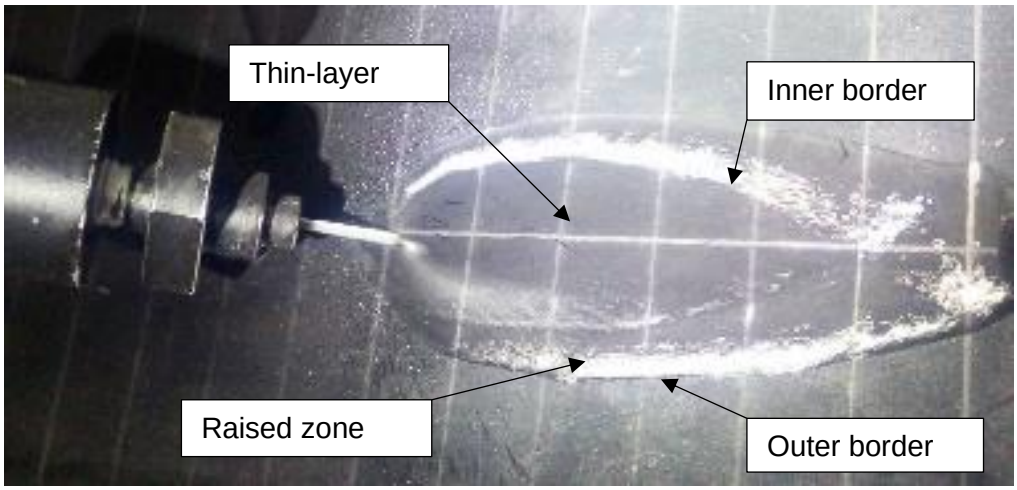

Figure 3. The top view of the film.

The raised zone is exactly the rim in the phenomena. In this experiment, the PLIF method is applied to reveal the rim. **Figure 4** is the processed photos that come from the PLIF method, which takes the cross-sectional photo of both the left and right rims of the film. The dot line is the centre symmetry line. It is found that the difference between the left and right rims is small. Therefore, only the right rim is researched in this paper. The solid line is the dividing line between the thin-layer zone and the rim.

Figure 4. The cross-sectional shape of both the left and the right of the film.

It is found that the rim will be thicker and wider when the rim is closer to the downstream. The shape of the rim has little change when the azimuthal angle, the impingement velocity, the impingement angle, the viscosity and the surface tension are different.

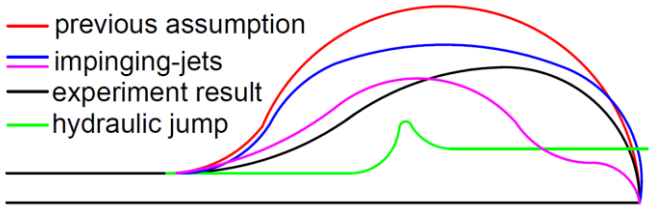

Figure 5. The diagrammatic drawing of cross-sectional right rim.

According to Yang[10], the rim in the previous assumption is drawn in **Figure 5** with red line. The red cross section is a standard semicircle, and the surface tension plays a key role in the case. According to Avedisian[11], the hydraulic jump is drawn in **Figure 5** with green line. The cross section is a sudden fluctuation, and the inertial force plays a key role in the case. According to McConley [7], the rim of the film formed by the impinging-jets are drawn in **Figure 5** with blue and purple line. The cross sections are oblate circle or peanut. Both the surface tension and the instability make different cross sections in the case. However, the cross section of the rim in this experiment seems like a half-leaf.

Semi-empirical model

Figure 6 is a hand-drawn axonometric view of a liquid film rim in a typical azimuthal angle γ. The film spreads from point O, which called the impingement point[12]. The liquid will pile up in the end, generating the rim, which is surrounded by the inner and outer border line.

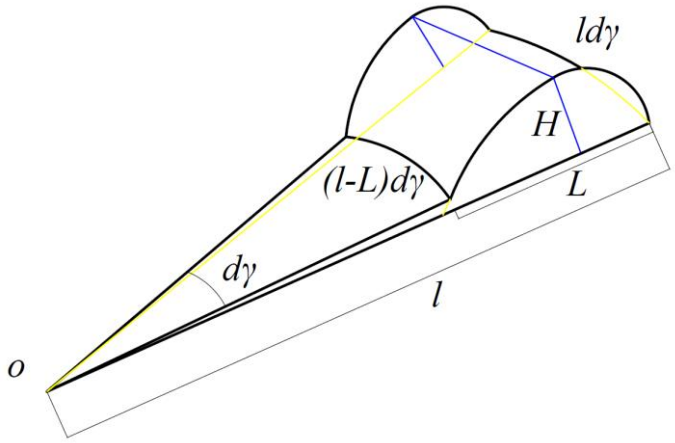

Figure 6. The hand-drawn axonometric view of a liquid film.

The width of the rim at azimuthal angle γ is the function of the distance L shown in **Figure 6**. The azimuthal angle $\gamma = 0$, when the direction of the flow tube is fully pointed downstream of the film.

The length l shown in **Figure 6**, is the distance of the stream tube at azimuthal angle γ. The rim thickness H shown in **Figure 6**, is between the highest point on the rim contour line and the point directly below. Moreover, the length of the unit volume that overlaps with the inner

border line is $(l-L)d\gamma$, and the length of the unit volume that overlaps with the outer border line is $ld\gamma$.

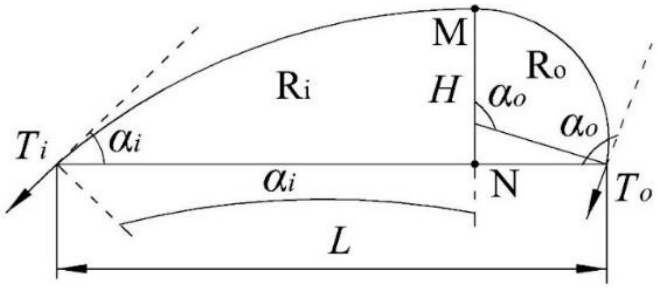

Figure 7. The circumferential cross section of the rim.

Based on **Figure 7**, the contour of the rim shape of the film can be considered as two arcs. Therefore, the shape of the rim can be divided into two parts, named part R_i and part R_o, by the pair of arcs which are shown in **Figure 7**.

Part R_o whose central angle of the profile is α_o, is close to the outer border line. Part R_i whose central angle of the profile is α_i, is close to the inner border line. The distance between the highest point M of the unit volume and the point N that is the projection of point M on the plate is H. The point M is just the highest point of both the R_o and R_i parts. Therefore, the direction of the surface tension ($T_i = \sigma_l(l-L)d\gamma$ and $T_o = \sigma_l l d\gamma$) of the pair of arcs can be obtained, as shown in **Figure 7**. The pressure difference Δp between the inside and the outside of the liquid rim can be expressed as

$$\Delta p = \rho_l g H \tag{1}$$

The pressure difference Δp is balanced by the surface tension T_i and T_o as

$$\Delta p \chi A = T_i sin\alpha_i + T_o sin\alpha_o \tag{2}$$

where the empirical parameter $\chi \approx 0.38 + 2.52\frac{\gamma}{\pi}$ shows the non-uniform distribution of the liquid in the rim.

The bottom area of the unit volume of the rim A is

$$A = \frac{(2l-L)d\gamma}{2} Lcos\frac{d\gamma}{2} \tag{3}$$

The element $d\gamma$ is so small that $\cos(d\gamma/2) \approx 1$. Ignoring small elements, the area is

$$A = (l-0.5L)Ld\gamma \approx lLd\gamma \tag{4}$$

where the length of streamline l, according to Wang [9].

Thus, the rim thickness H of the rim can be expressed as

$$H = \frac{T_i sin\alpha_i + T_o sin\alpha_o}{\rho_l g \chi A} \tag{5}$$

where the central angle $\alpha_o = \frac{\pi-\gamma}{4}$ and $\alpha_i = \frac{\pi-\gamma}{3}$.

Then, the geometric relationship of the rim cross-section shape shown in **Figure 7** is established as

$$L = \frac{Hsin\alpha_o}{1-cos\alpha_o} + \frac{Hsin\alpha_i}{1-cos\alpha_i} \quad (6)$$

in which the rim width L can be obtained.

Model validation and analysis

The exact thickness and width of the rim in the experiment while the azimuthal angle γ is 30°, 60°, 90°, 150°, are shown in **Figure 8** and **Figure 9**, respectively. Meanwhile, the prediction result of the semi-empirical model with the same operating conditions is also plotted in the same picture, for the benefit of the comparison.

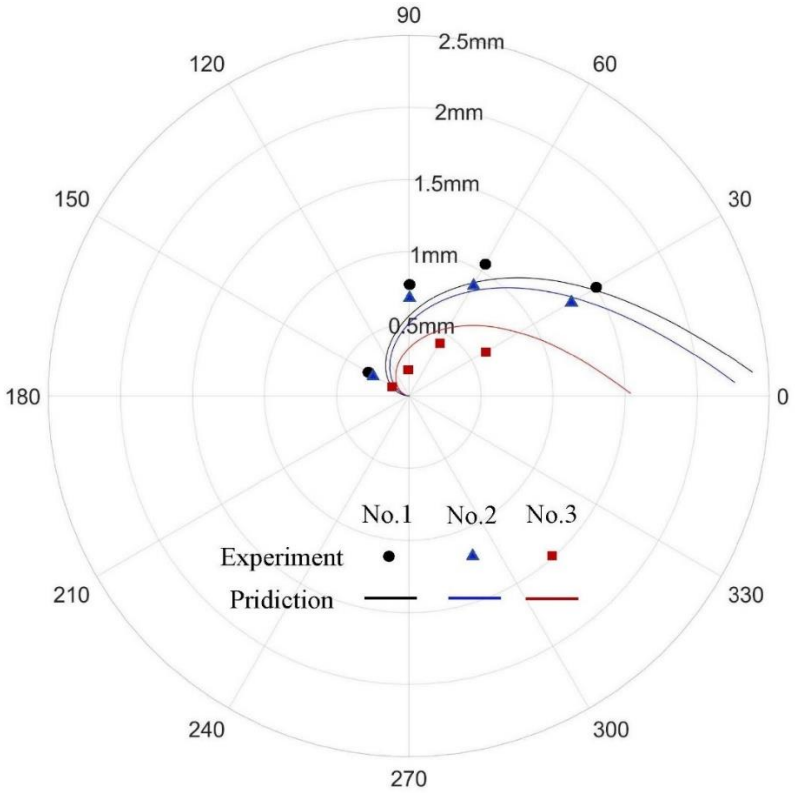

Figure 8. The thickness of the rim.

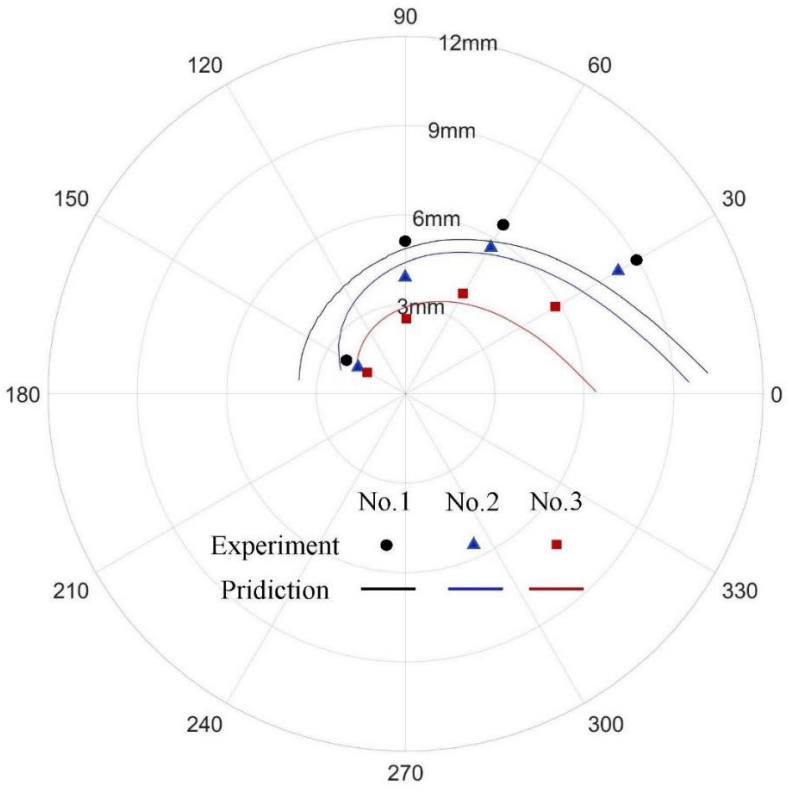

Figure 9. The width of the rim.

It is obvious that the law of the variation of both the thickness and width in the experiment is the similar as that comes from the semi-empirical model, when the azimuthal angle γ is between 30° and 150°. However, the relative error is unacceptable, when the azimuthal angle γ is in other positions.

According to the experiment, both the thickness and width of the rim are close to infinitesimal, when the angle is larger than 150°. At this very moment, the central angle α_o and α_i are linear no more.

According to the experiment, the width of the rim is keeping increasing, however, the thickness of the rim is keeping constant, when the angle is smaller than 30°. The surface tension of the liquid has reached the limit which it can withstand liquid mass no more.

Conclusions

The experiment with the liquid film generator is conducted. The typical shape of the rim is revealed, with the help of the PLIF method. According to the experiment, a semi-empirical model contained gravity, surface tension and viscosity simultaneously, is established, which has good accuracy.

- It is found by comparing the experimental phenomenon in this paper with other similar experimental phenomena that the cross-sectional shape of the rim is neither an assumed semicircle, nor the typical hydraulic jump, but an irregular leaf.
- The thickness and the width of rim that can be deduced by dividing the cross-sectional shape of the rim into two arcs with different curvatures, are expressed as $H = \frac{T_i sin\alpha_i + T_o sin\alpha_o}{\rho_l g \chi A}$ and $L = \frac{Hsin\alpha_o}{1-cos\alpha_o} + \frac{Hsin\alpha_i}{1-cos\alpha_i}$.

- Both the thickness and width of the rim are close to infinitesimal, when the angle is larger than 150°. The width of the rim is keeping increasing, however, the thickness of the rim is keeping constant, when the angle is smaller than 30°.

Nomenclature

γ	azimuthal angle [rad]
L	rim width [m]
T	surface tension [N]
H	rim thickness [m]
l	length [M]
α	central angle [°]
Δp	pressure difference [Pa]
χ	empirical parameter [-]
ρ	density [kg m^{-3}]
σ	surface tension coefficient [N m^{-1}]
A	area [m^2]
g	acceleration of gravity [m s^{-2}]

Acknowledgment

The financial support of Qian Xuesen youth foundation of China Aerospace Science and Technology Corporation is gratefully acknowledged.

References

[1] Choo Y, Kang B. A study on the velocity characteristics of the liquid elements produced by two impinging jets. Experiments in Fluids, 2003, 34(6), pp. 655-661.
[2] Lin Q, Yang C, Liu B. Effect of impingement angle and wall curvature on liquid film. Journal of national university of defense technology, 2013, 35(6), pp. 17-21.
[3] Donald L, Chubb DL, Calfo FD, et al. Geometry of thin liquid sheet flows. AIAA Journal, 1994, 32(6), pp. 1325-1328.
[4] Heidmann MF, Priem RJ, Humphrey JC. A study of sprays formed by two impinging jets. NACA Technical Notes, 1957, 3835.
[5] Watson EJ. The radial spread of a liquid jet over a horizontal plate. Journal of Fluid Mechanics 1964, 20(3), pp. 481–499.
[6] Bremond N, Villermaux E. Atomization by jet impact. Journal of Fluid Mechanics, 2006, 2006; 549(-1), pp. 273-306.
[7] Mcconley MW, Chubb DL, Mcmaster MS, et al. Stability of Thin Liquid Sheet Flows. Journal of Propulsion & Power, 1997, 13, pp. 74-81.
[8] Zang LY, Tian RF, Sun LX, et al. Application of planar laser-induced fluorescence technique in measurement of dynamic film thickness. Atomic Energy Science and Technology, 2014; 48(9), pp, 1654-1659.
[9] Wang RX, Huang Y, et al. Semi-empirical model for the engine liquid fuel sheet formed by the oblique jet impinging onto a plate. Fue, 2018, 233(DEC.1), pp, 84-93.
[10] Yang L, Zhao F, Fu Q, et al. Liquid sheet formed by impingement of two viscous jets. Journal of Propulsion & Power, 2014, 30(4), pp, 1016-1026.
[11] Avedisian CT, Zhao Z. The circular hydraulic jump in low gravity. Proceedings of the Royal Society A: Mathematical, Physical and Engineering Sciences, 2000, 2001:2127-2151.
[12] Hasson D, Peck RE. Thickness distribution in a sheet formed by impinging jets. AICHE Journal, 1964, 10(5), pp, 752–754.